TRENDS IN SCIENCES 2025; 22(8): 10057
https://doi.org/10.48048/tis.2025.10057 RESEARCH ARTICLE

Recombinant Bacteriocin Rhamnosin Suppresses Malignant Phenotypes of Colorectal Cancer Cells

Phonprapavee Tantimetta[1], Thanakrit Rattanaarchanai[1], Aratee Aroonkesorn[1,2], Wannarat Chanket[3], Phanthipha Runsaeng[1,2], Sittiruk Roytrakul[4], Pilaiwanwadee Hutamekalin[5] and Sumalee Obchoei[1,2,*]

[1]Department of Biochemistry, Division of Health and Applied Sciences, Faculty of Science, Prince of Songkla University, Hatyai, Songkhla 90110, Thailand
[2]Center of Excellence for Biochemistry, Faculty of Science, Prince of Songkla University, Hatyai, Songkhla 90110, Thailand
[3]Department of Chemistry, Faculty of Science, Silpakorn University, Nakhon Pathom 73000, Thailand
[4]Functional Proteomics Technology Laboratory, National Center for Genetic Engineering and Biotechnology, National Science and Technology Development Agency, Pathumtani 12120, Thailand
[5]Division of Health and Applied Sciences, Faculty of Science, Prince of Songkla University, Hatyai, Songkhla 90110, Thailand

([*]Corresponding author's e-mail: sumalee.o@psu.ac.th)

Received: 26 February 2025, Revised: 22 March 2025, Accepted: 29 March 2025, Published: 20 June 2025

Abstract

Colorectal cancer (CRC), the third most diagnosed cancer worldwide, is believed to worsened by microbiome dysbiosis, which promotes carcinogenesis through inflammation and genetic instability. Lactic acid bacteria (LAB), known for their beneficial metabolites, produce bacteriocins with potential anticancer properties. Here we hypothesized that recombinant rhamnosin (rRN), derived from the prebacteriocin gene of *Lactobacillus rhamnosus*, may inhibit CRC progression by targeting oncogenic pathways associated to proliferation, metastasis, and chemoresistance. We evaluated the anticancer activity of rRN in HT-29 and Caco-2 CRC cells, along with normal oral keratinocyte (NOK-SI) cells, using cell viability (MTT assay), apoptosis (Hoechst/propidium iodide dual nuclear staining), migration and invasion (Boyden chamber assay), and RT-qPCR to measure the expression of genes regulating growth, motility, and drug resistance. The results revealed that rRN dose-dependently inhibited CRC cell viability (IC_{50}: 25.3 and 14.5 µg/mL for HT-29 and Caco-2, respectively) with minimal toxicity to NOK-SI cells (IC_{50}: >32 µg/mL). When combined with 5-fluorouracil (5-FU), it enhanced the growth inhibitory effect. rRN induced apoptosis and suppressed migration and invasion by 70 - 80 %. Transcriptional profiling revealed the downregulation of genes related to cell growth (*CCNB1*, *CCND1* and *EGFR*), motility (*FN1*, *PXN* and *SNAI1*), and drug resistance (*ABCG2*, *MRP1* and *MRP2*), while *CCNE1* and *VIM* remained unaffected, underscoring rRN's selective targeting of CRC progression pathways. These findings establish rRN as a multitarget therapeutic candidate for CRC, addressing proliferation, metastasis, and chemoresistance - key challenges in CRC relapse. Future studies should validate protein-level mechanisms, such as caspase activation and BCL-2/Bax dynamics, and evaluate rRN's efficacy in preclinical models. This work underscores the potential of rRN, a LAB-derived bacteriocin, as a novel adjuvant for CRC treatment.

Keywords: Bacteriocins, Lactic acid bacteria, *Lactobacillus rhamnosus*, Recombinant rhamnosin, Colorectal cancer, anticancer, Cell proliferation, Cell motility, Apoptosis

Introduction

As the third most diagnosed cancer and the second leading cause of cancer-related mortality, colorectal cancer (CRC) raises the major global health concerns. Recent estimates indicate over 935,000 fatalities in 2020 alone [1,2]. CRC risk arises from genetic predisposition, environmental influences, and lifestyle choices [3]. Surgery and radiation are the main treatment options for early-stage CRC, while chemotherapy is commonly used for treating advanced CRC [4]. Over time, cancer cells can acquire resistance to chemotherapy, ultimately rendering the treatment ineffective [5]. Beyond resistance, chemotherapeutic drugs often cause significant side effects, highlighting the need to search for alternative treatments that are more effective and safer [6].

In the past decade, research on gut microbiota has expanded, revealing its essential role in maintain gut health under both physiological and pathological conditions [3]. An imbalanced gut microbiota, also known as dysbiosis, results in the production of toxic metabolites, leading to inflammation, DNA damage and drug resistance. In CRC, dysbiosis-driven inflammation and DNA damage are key contributors to tumorigenesis and chemoresistance [3]. Beneficial bacteria, including lactic acid bacteria (LAB), contribute to a balanced gut microbiome by maintaining gut barrier integrity, regulating metabolism, and modulating immune responses. LAB, a group of lactic acid-producing Gram-positive bacteria, are naturally found in healthy guts and fermented foods [7]. These bacteria not only contribute to gut homeostasis but are also classified as Generally Recognized as Safe (GRAS) due to their extensive history of use in food production [8]. LAB can produce numerous beneficial active metabolites, such as organic acids, short-chain fatty acids, and bacteriocins. In CRC, LAB-derived metabolites like bacteriocins may counteract dysbiosis-associated carcinogenesis by restoring microbiome balance and targeting cancer cells [9].

Bacteriocins are antimicrobial peptides produced by bacteria to inhibit the colonization and growth of competitive bacteria of closely related species. They can have a narrow or broad spectrum of activity. Like most proteins in cells, bacteriocins are synthesized on ribosomes through the process of translation [10, 11]. Bacteriocin from Gram-positive bacteria are categorized into 4 classes based on structure and function. Class I (lantibiotics, e.g., nisin) are small, post-translationally modified peptides. Class II (non-lantibiotics) are heat-stable, unmodified peptides subdivided into pediocin-like, two-peptide, circular, and linear bacteriocins. Class III comprises large, heat-labile bacteriolysins, while Class IV includes lipid- or carbohydrate-containing bacteriocins [12].

Due to their safety profiles and health benefits, bacteriocins have been extensively explored as potential anticancer agents. Many studies have found that bacteriocins exhibit promising anticancer effects and selective cytotoxicity against cancer cells while having minimal toxicity toward normal cells. The reported mechanisms include destabilization and disruption of the cancer cell membrane [13], induction of apoptosis, and cell cycle arrest [14]. Some bacteriocins have been shown to inhibit the metastatic process of cancer cells. For instance, nisin, a lantibiotic from *Lactococcus lactis*, induces apoptosis in head and neck cancer cells and reduces tumor burden in a mouse model. It also inhibits the growth of breast and colorectal cancer cells [15]. Similarly, pediocin PA-1 from *Pediococcus acidilactici* suppresses lung (A-549) and colon (DLD-1) cancer cell lines [13, 16]. Additionally, plantaricin A from Lactobacillus plantarum shows apoptosis induction effects on leukemia cells [13, 17].

In our previous study, we successfully produced and purified recombinant rhamnosin (rRN) from the prebacteriocin gene of *Lactobacillus rhamnosus* and assessed its anticancer activity against cholangiocarcinoma (CCA) cell lines. The key findings include rRN significantly suppressing cell growth, inducing apoptosis, and enhancing CCA cell sensitivity to gemcitabine [18]. In this study, we further explore the effects of rRN on various cancer phenotypes in CRC cell lines HT-29 and Caco-2, including cell growth, apoptosis, migration, invasion, and chemosensitivity. Moreover, we examine the expression of key genes in relevant pathways.

Materials and methods

Gene synthesis and plasmid construction

The recombinant rhamnosin (rRN) expression plasmid (pET29a_rRN) was constructed using an established method previously described [18]. Firstly,

the prebacteriocin gene sequence from *Lactobacillus rhamnosus* was retrieved from the NCBI database (accession number KY355775). Then, the sequence was optimized for expression in *Escherichia coli*; specifically, the codon usage of the gene was adjusted to match the preferred codons of the host organism. The optimized gene sequence, consisting of 351 base pairs, was synthesized by GenScript® (DE, USA). This sequence was subsequently cloned into the pET29a (Novagen®, UK) at the *Bam*HI and *Xho*I restriction sites, immediately upstream of a hexahistidine (6×His) tag sequence positioned at the C-terminus of the protein to facilitate downstream purification. The integrity and accuracy of the expression vector were verified by DNA sequencing to ensure proper insertion and the correct reading frame.

Expression of rRN in *E. coli*

The bacterial expression system was used for rRN expression as previously described [18]. In brief, the pET29a_rRN expression plasmid was transformed into competent *Escherichia coli* BL21 Star™ (DE3) cells using the heat shock transformation method. The transformed clones were selected on Luria-Bertani (LB) medium with 50 μg/mL kanamycin added. For rRN expression, a transformed colony was picked and cultured in LB medium at 37 °C with continuous shaking. When the optical density at 600 nm (OD_{600}) reached 0.6 - 0.8, the bacterial cells were induced with 0.1 mM isopropyl β-D-1-thiogalactopyranoside (IPTG) to initiate protein expression. The culture was then incubated for 16 h at 25 °C with continuous shaking. After incubation, the cells were harvested for downstream assays or protein purification.

Purification of rRN

For rRN purification, the cells from the expression step were harvested by centrifugation at 6,000× g for 5 min, washed twice, and resuspended in 20 mM HEPES, pH 7.4. Then, the cells were lysed using repeated freeze-thaw cycles coupled with ultrasonication using a Sonics Vibra-Cells VCX-500 (Artisan Technology Group®, USA). The cell lysate was centrifuged at 15,000× g for 30 min, the supernatant was collected and loaded into a pre-equilibrated Ni^{2+}-nitrilotriacetic acid (Ni-NTA) HisTrap™ HP column. Finally, the bound rRN protein was eluted with elution buffer, dialyzed, and desalted using a 3 kDa cutoff ultrafiltration membrane (Amicon, Merck, Germany) and column chromatography (Sephadex G-25 in PD-10, GE Healthcare, UK), respectively.

Protein determination using BCA assay

To measure protein concentrations, the microplate method of the Bicinchoninic Acid (BCA) assay (Thermo Scientific, USA) was performed following the supplier's instructions. The working BCA reagent was prepared by mixing reagent A and reagent B in a 50:1 ratio. The standard protein, bovine serum albumin (BSA), and protein samples were diluted into suitable concentrations. Then 25 μL of those were added to a 96-well microplate, followed by 200 μL of the working BCA reagent. The plate was incubated at 37 °C for 30 min, then allowed to cool to room temperature for 10 - 15 min before measuring absorbance at 562 nm using a microplate reader (Spark® Multimode Microplate Reader, Tecan, Switzerland). For protein concentration estimation, a standard curve was first generated by plotting BSA absorbance values against their concentrations. Then the standard curve was used to quantify the protein concentration of the protein samples by comparing their absorbance values to the standard curve.

SDS-PAGE

Protein samples were analyzed based on their molecular weight through separation by sodium dodecyl sulfate-polyacrylamide gel electrophoresis (SDS-PAGE). Firstly, a 30 % acrylamide and 0.8 % bis-acrylamide mixed solution was prepared and then used to generate 12 % resolving and 5 % stacking polyacrylamide gels by mixing with 0.1 % SDS and Tris-HCl buffer, 1.5 M, pH 8.8, and 0.5 M, pH 6.8, for the resolving gel and stacking gel, respectively. To initiate gel polymerization, 0.05 % ammonium persulfate (APS), and 0.05 % tetramethylethylenediamine (TEMED) were added. Protein samples were prepared by mixing with Laemmli sample buffer containing 5 % β-mercaptoethanol, then heated at 95 °C for 5 min. A protein molecular weight marker and the treated samples were loaded into the gel and electrophoresed at 120 V in Tris-glycine running buffer for 45 min. Then, the gel was stained with Coomassie Brilliant Blue R-250 for 2 h and soaked in a

destaining solution (40 % methanol, 10 % acetic acid) until the protein bands became prominent and the background was clear.

Cell viability assay

To evaluate the cell growth inhibitory effect of rRN against CRC cells, a cell viability assay using the 3-(4,5-dimethylthiazol-2-yl)-2,5-diphenyltetrazolium bromide (MTT) test was performed. Firstly, CRC cells (HT-29 and Caco-2), as well as the normal NOK-SI cell line, were seeded into a 96-well plate at a density of 2×10^3 cells per 100 µL per well, then incubated for 24 h to allow attachment. The next day, the cells were treated with various concentrations of rRN (0, 2, 4, 6, 8, 16 and 32 µg/mL) for 72 h and subjected to MTT assay. In brief, 20 µL of MTT reagent (5 mg/mL) was added to each well, incubated for 2 h at 37 °C. Excess MTT was removed, and the purple formazan crystals were dissolved by adding 100 µL of DMSO. Then absorbance was measured at 540 nm using a microplate reader to determine cell viability.

The MTT assay was also applied to determine the effect of combined 5-fluorouracil (5-FU) and rRN treatment. First, HT-29, Caco-2, and NOK-SI cells were treated with various concentrations of 5-FU for 72 h, followed by the MTT assay. The IC_{50} values were calculated. For the combination treatment, the sub-IC_{50} concentrations of 5-FU for each cell line were selected. HT-29 and Caco-2 cells were seeded overnight. The following day, cells were treated with various concentrations of rRN alone or combined with sub-IC_{50} concentrations of 5-FU (50 µM for HT-29 and 25 µM for Caco-2, respectively) for 72 h. These combination treatments were also performed in NOK-SI for comparison. Finally, the MTT assay was then performed to assess cell viability as described above.

Apoptotic nuclear staining

Apoptotic nuclear staining was performed on HT-29 and Caco-2 cell lines following treatment with rRN. First, cells were seeded at a density of 2×10^5 cells per well in a 6-well plate and incubated overnight to allow attachment. The following day, cells were treated with rRN at concentrations of 0, 8, 16 and 32 µg/mL for 72 h. After treatment, cells were incubated with propidium iodide (PI) and Hoechst 33342 for dual nuclear staining. Hoechst 33342, a cell-permeable dye, stains the DNA of both live and dead cells, while PI, a membrane-impermeable dye, stains only the DNA of dead cells with compromised membranes. Therefore, nuclei stained with both dyes were considered dead or apoptotic. Stained cells were observed and imaged under a fluorescence microscope, apoptotic and total nuclei were counted from 5 randomly selected low-power fields, then calculated and presented as percentage of apoptotic nuclei.

Boyden chamber cell migration and invasion assay

To assess the effects of rRN on cancer cell motility (cell migration and cell invasion), Boyden chamber assays were performed. To observe these phenotypes without confounding effects from cell growth inhibition, relatively low concentrations of rRN (4 and 8 µg/mL), which do not affect cell viability at 24 h, were chosen. HT-29 and Caco-2 cells were trypsinized and counted, and then 2×10^4 cells were mixed with 0, 4 or 8 µg/mL rRN in 200 µL of serum-free medium (SFM). The cell suspension mixtures were added to 8.0 µm porous Transwell inserts, also known as the upper chamber. As a chemoattractant, a total of 800 µL of complete medium was added to the lower chamber. Similar steps were performed for the invasion assay; however, before seeding the cells, the Transwell inserts were precoated with 0.5 mg/mL Matrigel (Corning Life Sciences, Bedford, MA, USA) and incubation for 2 h at 37 °C. In both assays, the cells were incubated for 20 h, allowing them to migrate or invade through the membrane into the lower chamber. After incubation, non-migrated or non-invaded cells on the upper surface of the membrane were removed with a cotton swab. Then, the migrated and invaded cells on the lower surface of the membrane were fixed with 4 % paraformaldehyde and stained with 0.4 % sulforhodamine B. The stained cells were observed under a microscope and counted in 6 randomly selected low-power fields.

RNA isolation and RT-qPCR

Total RNA was extracted from rRN-treated HT-29 and Caco-2 cells using Trizol reagent. Next, 2 µg of total RNA was reverse-transcribed to cDNA using the RevertAid First Strand cDNA Synthesis Kit (Thermo Fisher Scientific, Waltham, MA, USA). Dye-based quantitative PCR (qPCR) was performed with PanGreen

Universal SYBR Green Master Mix (2X) (Bio-Helix, Taiwan) using gene- specific primers, with Glyceraldehyde-3-Phosphate Dehydrogenase (*GAPDH*) as the internal control. The sequences of the primers are presented in **Table 1**. The qPCR was performed using the following thermal cycling conditions: An initial denaturation at 95 °C for 15 min, followed by 35 cycles of denaturation at 95 °C for 20 s, annealing at 60 °C for 1 min, and extension at 72 °C for 2 min. Reactions were conducted using the Stratagene Mx3005P (Agilent Technologies, Santa Clara, USA). Gene expression levels were determined using the relative quantification method via the $2^{-\Delta\Delta Ct}$ equation.

Table 1 List of primers.

Gene		Sequence (5′ to 3′)	Amplicon length (bp)
GAPDH	Forward:	CAAATTCCATGGCACCGTCA	132
	Reverse:	GACTCCACGACGTACTCAG	
CCNB1	Forward:	ATGCAGCACCTGGCTAAGAAT	118
	Reverse:	TCAGCTGTGGTAGAGTGCTG	
CCND1	Forward:	GATGCCAACCTCCTCAACGA	163
	Reverse:	ACTTCTGTTCCTCGCAGACC	
CCNE1	Forward:	TGTGTCCTGGATGTTGACTGCC	123
	Reverse:	CTCTATGTCGCACCACTGATACC	
EGFR	Forward:	TTGCCGCAAAGTGTGTAACG	112
	Reverse:	GAGATCGCCACTGATGGAGG	
FN1	Forward:	AGGAGAATGGACCTGCAAGC	159
	Reverse:	GAAGTGCAAGTGATGCGTCC	
PXN	Forward:	AGCCTCAGTCCTCATCACCT	165
	Reverse:	TCATTACGGTGGGTGAAGGC	
SNAI1	Forward:	TCTCTTCCTTGGAGGCCGA	174
	Reverse:	GGCTTCGGATGTGCATCTTG	
VIM	Forward:	GGACCAGCTAACCAACGACA	178
	Reverse:	AAGGTCAAGACGTGCCAGAG	
ABCG2	Forward:	TTCGGCTTGCAACAACTATG	128
	Reverse:	TCCAGACACACCACGGATAA	
MRP1	Forward:	TTCTGGCTGGTAGCCCTAGT	192
	Reverse:	GTCGTGGATGGTTTCCGAGA	
MRP2	Forward:	GCAGACCTGCCACTTTGTTT	164
	Reverse:	AGAAAACCAACGAATACCTGCT	

Results and discussion

Expression and purification of rRN

In this study, we successfully expressed recombinant rRN using the pET29a_rRN construct in *E. coli* BL21 Star™ (DE3) cells and purified it using Ni-NTA affinity chromatography. The expression results revealed that rRN was predominantly produced in a soluble form, facilitating efficient downstream purification and eliminating the need for complex refolding steps required for proteins expressed in inclusion bodies. The molecular mass of ~16 kDa was observed on SDS-PAGE, which was consistent with its predicted size, confirming its correct expression and successful purification (**Figure 1(B)**). The successful production of soluble rRN provides a crucial foundation for its functional characterization in subsequent assays [19]. Future work may involve optimizing yield and exploring large- scale production strategies for therapeutic applications.

Table 2 The half-maximal inhibitory concentrations (IC_{50}) of rRN and 5-FU.

Cell lines	IC_{50}	
	rRN (μg/mL)	5-FU (μM)
NOK-SI	> 32	NA
HT-29	25.3 ± 0.32	66.9 ± 3.57
Caco-2	14.5 ± 0.35	44.9 ± 3.10

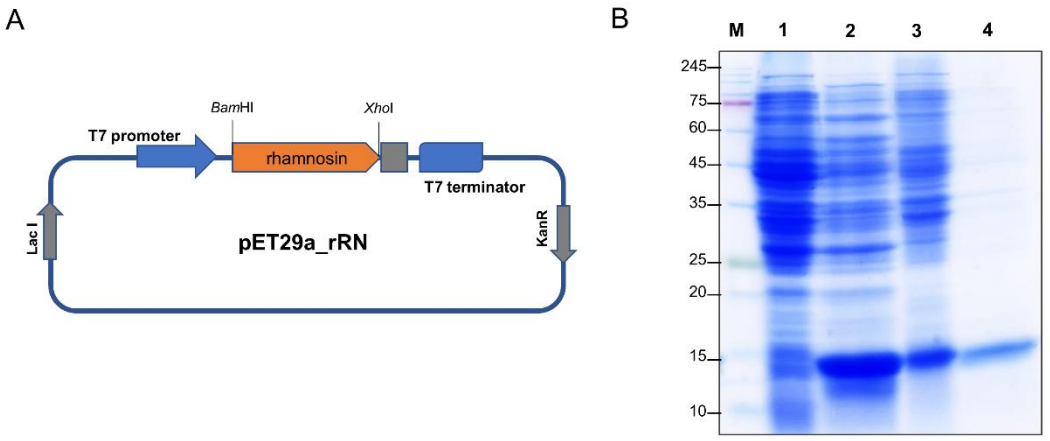

Figure 1 Expression of rRN. (A) pET29a_rRN expression plasmid map. (B) SDS-PAGE analysis. Lane M: Protein molecular weight markers; lane 1: Uninduced bacterial cell lysate; lane 2: Induced cell lysate (soluble fraction); lane 3: Induced cell lysate (insoluble fraction); lane 4: purified recombinant bacteriocin.

Colorectal cancer cell growth is inhibited by rRN

An MTT assay was performed to evaluate the cell growth inhibitory effect of rRN on CRC cells. Two human CRC cell lines, HT-29 and Caco-2, along with normal NOK-SI cells, were treated for 72 h with various concentrations of rRN. The results showed that rRN suppressed the growth of the CRC cell lines in a dose-dependent manner, with a stronger effect observed in Caco-2 cells (**Figure 2(A)**). In contrast, NOK-SI cells were well-tolerant of rRN treatment. The IC_{50} values at 72 h were 14.5 ± 0.35 μM for Caco-2, 25.3 ± 0.32 μM for HT-29, and > 32 μM for NOK-SI (**Table 2**).

The strong growth-inhibitory effect of rRN against CRC cells and its low toxicity to normal cells align with previous studies on bacteriocins derived from *Lactobacillus* spp., which have shown selective anticancer properties by targeting cancer cells with minimal impact on normal cells [13, 20]. Additionally, our earlier research on cholangiocarcinoma found similar cancer cell-selective cytotoxicity with rRN [18]. These results suggest that rRN may serve as a promising therapeutic agent that could reduce the side effects commonly associated with conventional chemotherapies.

The distinct differences in membrane characteristics between normal and cancer cells may contribute to the selective action of bacteriocins. As many bacteriocins are highly positively charged peptides, while cancer cell membranes are typically more negatively charged, more fluid, and have a higher density of microvilli compared to normal cells—which have a neutral charge and structured lipid layers—these differences may explain their selective cytotoxicity [21-23]. These properties make cancer cells more susceptible to the binding and destabilization effects of bacteriocins [24].

Effect of 5-Fluorouracil is enhanced by rRN

The 5-Fluorouracil (5-FU) is a first-line chemotherapeutic drug commonly used in the treatment of many cancers, including CRC. However, treatment often fails due to the acquired resistance of cancer cells. Additionally, chemotherapeutic drugs are known for

their side effects. We aimed to test whether rRN could enhance the effect of 5-FU; therefore, a combination treatment was conducted. First, an MTT assay was performed on HT-29 and Caco-2 cells treated with various concentrations of 5-FU. The results showed that 5-FU decreased cell viability in both cell lines in a dose-dependent manner, with a stronger effect observed in Caco-2 cells (**Figure 2(B)**). The calculated IC_{50} values were 66.9 ± 3.57 μM for HT-29 and 44.9 ± 3.10 μM for Caco-2 (**Table 2**). Subsequently, combination treatment was conducted by treating cells with various concentrations of rRN with or without 5-FU (50 μM for HT-29 and 25 μM for Caco-2). After 72 h of treatment, the MTT assay was performed, and the results indicated that cells treated with the combined rRN and 5-FU showed a significantly stronger cytotoxic effect than those treated with either rRN or 5-FU alone.

These findings suggest that rRN could enhance the effect of 5-FU when used in combination. This synergistic effect may result from rRN enhancing CRC cells' chemosensitivity, which could allow for lower doses of 5-FU to achieve similar therapeutic effects, while minimizing the adverse effects associated with higher chemotherapeutic drug doses [18, 25]. However, to fully translate these findings into clinical applications, future studies must address the safety profile of this combination therapy. Although the reduced 5-FU dosage suggested here may theoretically mitigate systemic toxicity, the selectivity of rRN toward cancer cells over normal cells remains unvalidated. Specifically, assays using non-cancerous cell lines are required to explicitly evaluate whether the lower rRN dose in combination with 5-FU preserves selectivity for cancer cells and to quantify any residual off-target effects that could confirm minimal harm to normal tissues. These studies will ensure that the therapeutic window - balancing efficacy against CRC cells with safety for healthy cells - is adequately defined. This finding supports previous reports that bacteriocins can sensitize cancer cells to chemotherapeutic agents, improving treatment outcomes [14].

rRN induces apoptosis in HT-29 and Caco-2 cells

An apoptosis assay is often used to evaluate the effectiveness of anticancer agents by measuring apoptotic cells in response to treatment. To examine the hypothesis that rRN induces apoptotic cell death, CRC cells were treated with rRN at concentrations of 8, 16 and 32 μg/mL for 72 h, alongside untreated control cells. Nuclear double staining using propidium iodide and Hoechst 33342 revealed that relatively high concentrations of rRN (16 and 32 μg/mL) led to a dose-dependent increase in apoptotic nuclei in HT-29 (**Figure 3(A)**) and Caco-2 cells (**Figure 3(B)**). Notably, cells treated with 8 μg/mL did not exhibit significant apoptosis induction compared to negative controls. In addition to apoptotic induction, treatment groups (doses > IC_{50}) displayed reduced cell numbers and enlarged cell morphology (**Figure 3(B))**, potentially reflecting cellular stress responses (e.g., transient swelling or senescence-like phenotypes) or optical artifacts from reduced cell density.

The induction of apoptosis by rRN suggests that it may act as a cytotoxic agent targeting apoptosis pathways in CRC cells, potentially helping to overcome resistance mechanisms in these cells [14]. This observation is consistent with our previous report, which showed that rRN induced apoptosis in cholangiocarcinoma cells [18] and other studies demonstrating that bacteriocins can trigger apoptosis in various cancer cell types by disrupting cellular signaling pathways and inducing pro-apoptotic factors [13,15]. The observed enlargement of treated cells (**Figure 3(B)**) may represent early stress responses (e.g., senescence or cytoskeletal reorganization) preceding apoptosis, though optical artifacts from sparse cell populations cannot be ruled out. Further studies assessing senescence markers or cytoskeletal dynamics are warranted to clarify this phenomenon.

rRN attenuates migration and invasion of colorectal cancer cells

Cell migration and invasion are critical malignant phenotypes required for tumor metastasis; therefore, suppressing the migration and invasion abilities of cancer cells can slow tumor progression. To assess the inhibitory effect of rRN on these cell motility phenotypes, HT-29 and Caco-2 cells were treated with 0, 4 and 8 μg/mL of rRN and then subjected to Boyden chamber migration and invasion assays. Treatment with rRN significantly and dose-dependently reduced the migration capacity of HT-29 cells (**Figure 4(A)**). Additionally, cell invasion was significantly suppressed

by rRN; however, the inhibitory effect did not differ significantly between the 4 and 8 μg/mL treatments (**Figure 4(C)**). In Caco-2 cells, rRN significantly suppressed both cell migration and invasion in a dose-dependent fashion (**Figure 4(B)** and **4(D)**). Furthermore, at concentrations of 4 and 8 μg/mL, rRN did not exhibit any growth-inhibitory effect on either cell line after 24 h (**Figure 4(E)**).

Taken together, the Boyden chamber assays demonstrated that rRN effectively suppressed the migration and invasion capabilities of CRC cells, even at relatively low doses, ensuring that the reduced cell motility was not caused by growth inhibition. As cancer cell motility is a significant characteristic of cancer metastasis, its inhibition by rRN could substantially hinder cancer progression [26]. Bacteriocins are known for their anti-metastatic properties, which involve interfering with cancer cell adhesion, motility, and invasion pathways [15, 27, 28]. The inhibition of cell motility by rRN supports the potential of bacteriocins as therapeutic agents targeting not only primary tumor growth but also metastatic spread [15].

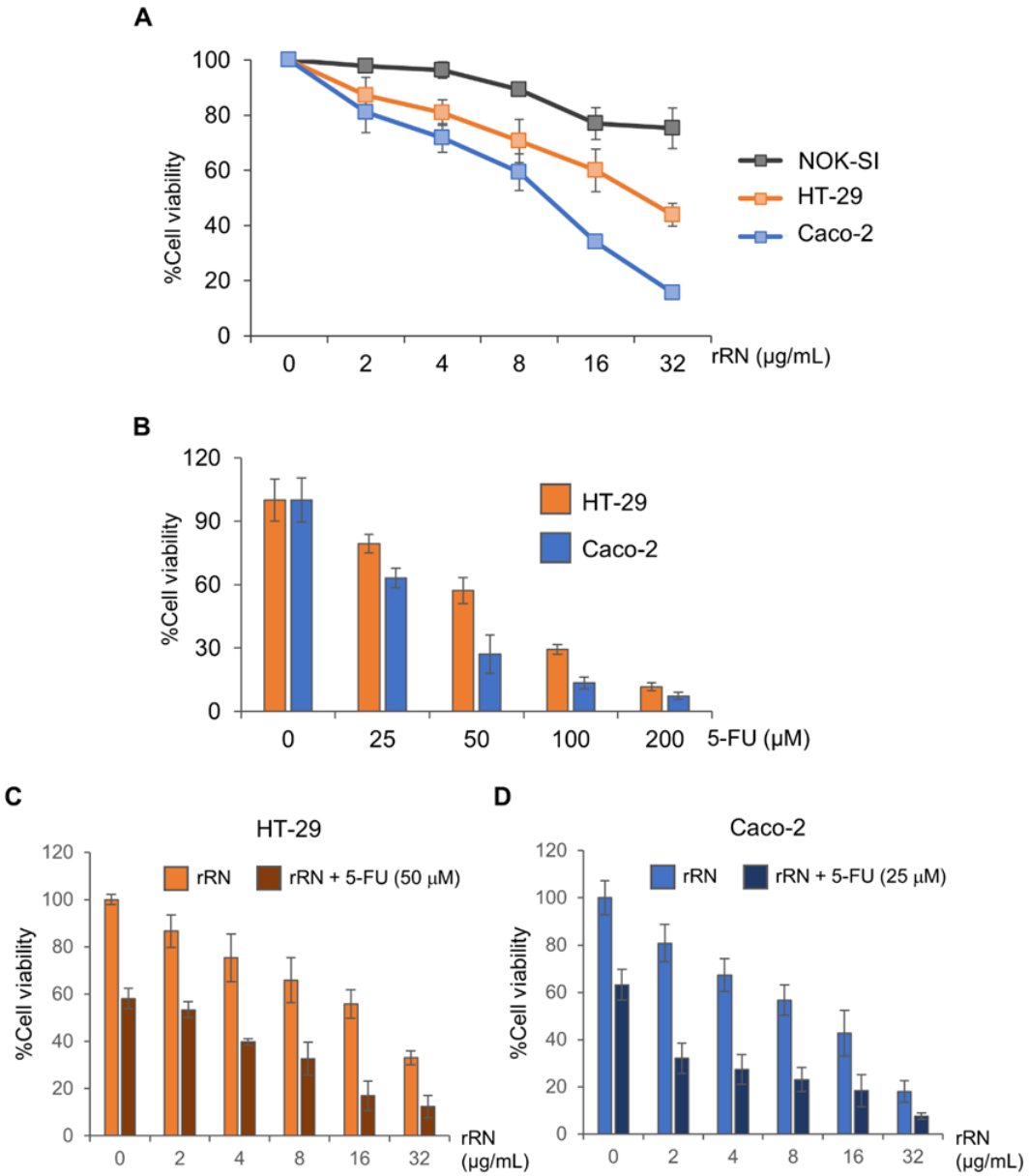

Figure 2 Effect of rRN on CRC cell viability as a single agent and in combination with 5-FU. (A) Cell viability of HT-29, Caco-2, and normal cell lines after treatment with rRN for 72 h. (B) Cell viability of HT-29 and Caco-2 cells after treatment with 5-FU for 72 h. Combined rRN and 5-FU treatment in (C) HT-29 and (D) Caco-2 cells.

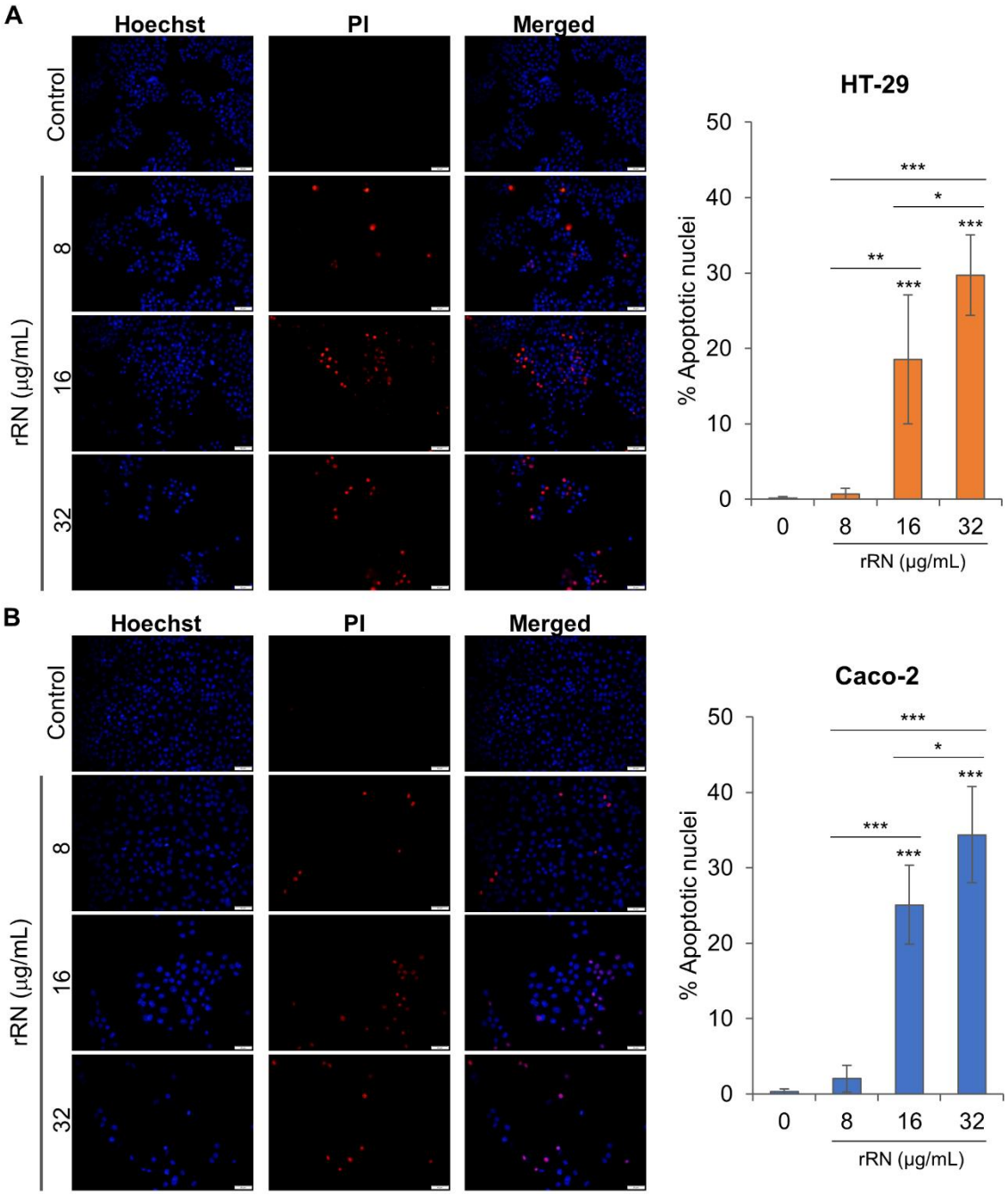

Figure 3 Apoptotic nuclear staining after treatment with rRN. (A) HT-29 and (B) Caco-2 cells after treatment with rRN for 72 h were subjected to double nuclear staining. Representative images of stained cells were captured via fluorescence microscope (left), and the graph represents the percentage of apoptotic nuclei (right). Significant differences are indicated by $^{*}p < 0.05$, $^{**}p < 0.01$, and $^{***}p < 0.001$.

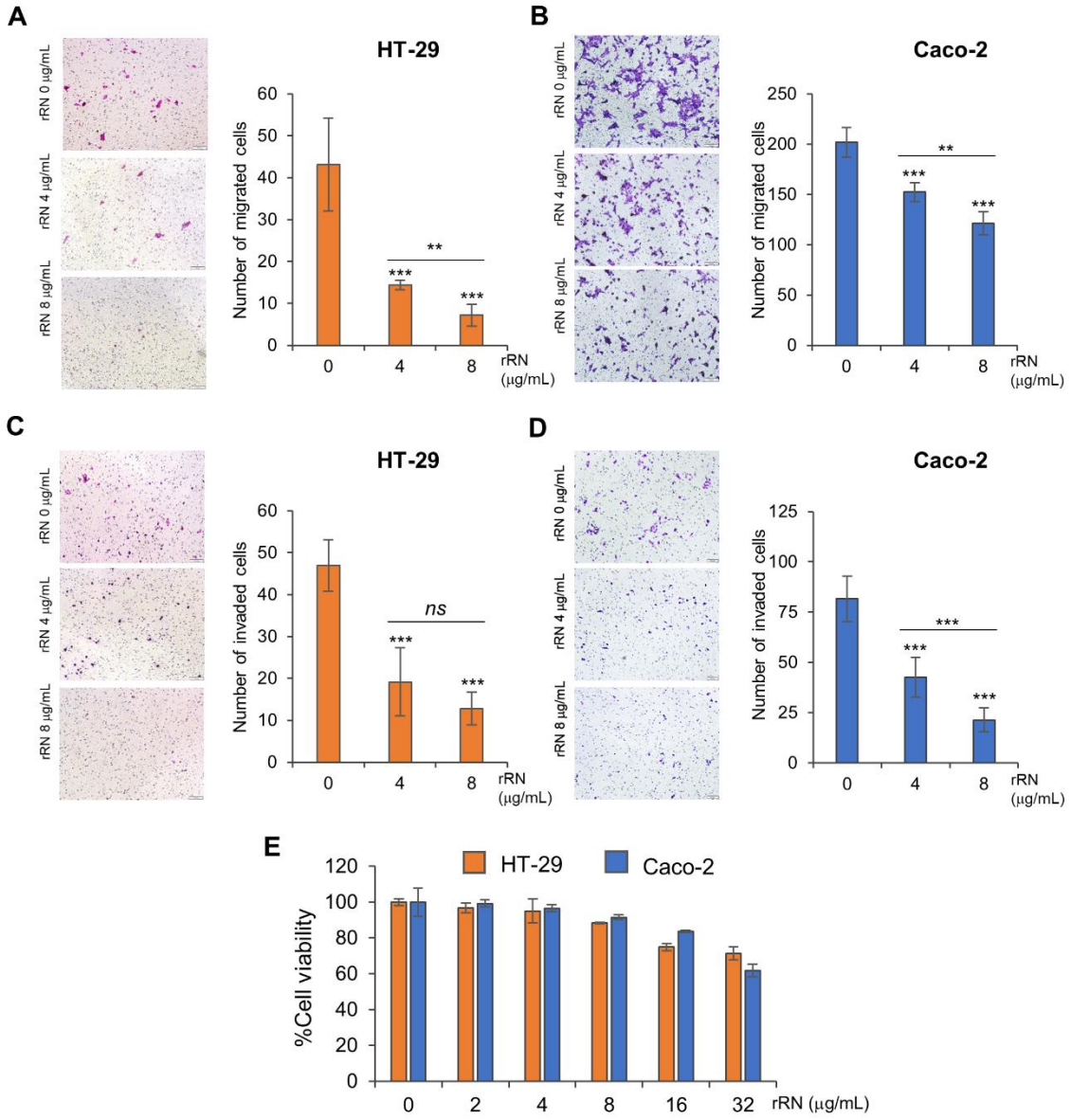

Figure 4 Effect of rRN on cell motility in CRC cell lines. Cell migration assay in HT-29 (A) and Caco-2 (B) cells. Cell invasion assay in HT-29 (C) and Caco-2 (D) cells. (E) Cell viability assay after rRN treatment for 24 h. Significant differences are indicated by $^{**}p < 0.01$ and $^{*}p < 0.001$; ns, not significant.

rRN suppresses key regulatory genes related to malignant phenotypes in of CRC cells

We observed that rRN significantly attenuates cell growth, cell motility, and drug-resistant phenotypes in colorectal cancer cell lines. Subsequently, RT-qPCR was performed to analyze the influence of rRN treatment on the mRNA expression of key genes related to cell growth (*CCNB1*, *CCND1*, *CCNE1* and *EGFR*), cell motility (*FN1*, *PXN*, *SNAI1* and *VIM*), and drug resistance (*ABCG2*, *MRP1* and *MRP2*). The results revealed that rRN at concentrations of 16 and 32 μg/mL significantly and dose-dependently inhibited the mRNA expression of *CCNB1*, *CCND1* and *EGFR* in HT-29 cells. In contrast, in Caco-2 cells, the expression of these genes was significantly suppressed only at 32 μg/mL of rRN. Additionally, rRN exhibited minimal to no effect on *CCNE1* expression in both cell lines (**Figure 5(A)**). Treatment with low concentrations of rRN (4 and 8 μg/mL) for 24 h significantly suppressed the expression of cell motility-related genes (*FN1*, *PXN* and *SNAI1*), while showing minimal to no effect on *VIM* expression (**Figure 5(B)**). Furthermore, rRN strongly suppressed

the mRNA expression of drug-resistance-related genes, including *ABCG2*, *MRP1* and *MRP2*, in the HT-29 cell line. In the Caco-2 cell line, MRP1 and MRP2 were significantly suppressed by rRN treatment, whereas ABCG2 expression remained unaffected (**Figure 5(C)**).

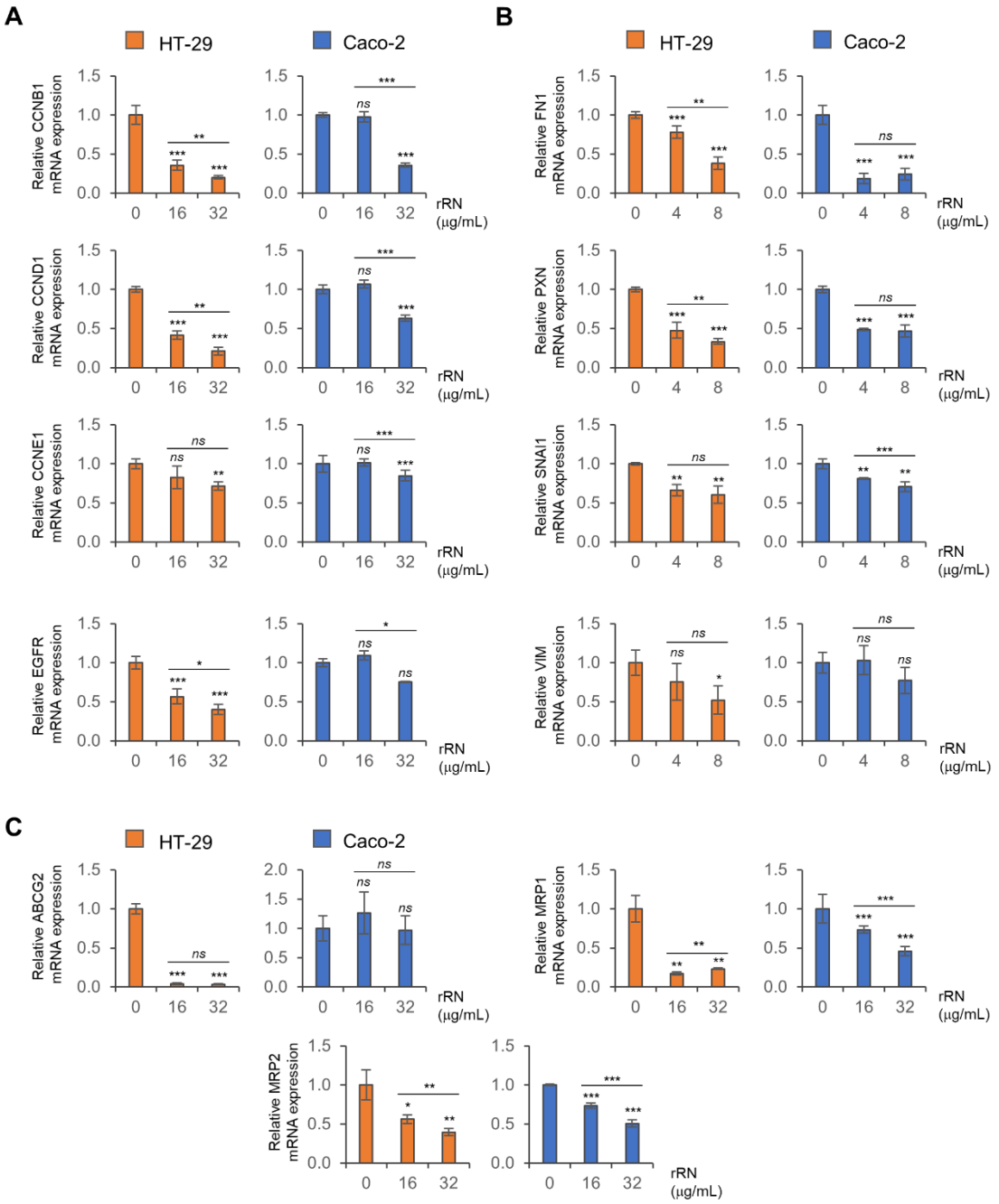

Figure 5 Gene expression analysis using RT-qPCR. Expression of genes related to (A) cell growth, (B) cell motility, and (C) drug resistance. Significant differences are indicated by $^{*}p < 0.05$, $^{**}p < 0.01$, and $^{*}p < 0.001$; ns, not significant.

The results of this study demonstrate the potential of rRN as an effective suppressor of malignant phenotypes in CRC cells by targeting key regulatory genes. The observed dose-dependent inhibition of *CCNB1*, *CCND1*, and *EGFR* suggests that rRN impairs cell growth by disrupting cell cycle and growth signaling pathways, consistent with the established roles of these genes in CRC progression and proliferation. Interestingly, the minimal impact on *CCNE1* indicates selective targeting of specific growth regulators; an in-depth study may provide insights into the precise molecular mechanisms of rRN action. CCND1 (Cyclin

D1) and CCNE1 (Cyclin E1) play a crucial role in regulating the G1 to S transition of the cell cycle, with Cyclin D1 activating CDK4/6 and Cyclin E1 activating CDK2. The *CCNB1* gene encodes Cyclin B1, a regulatory protein involved in the cell cycle. It can form a complex with CDK1 (Cyclin-dependent kinase 1) to regulate the transition from the G2 phase to mitosis. Aberrant expression of these cell cycle regulatory proteins is linked to uncontrolled proliferation in cancers [29]. Epidermal growth factor receptor (EGFR) is a transmembrane receptor tyrosine kinase that regulates cell proliferation, survival, migration, and differentiation through various signaling pathways. Overactivation of EGFR is commonly observed in many cancers and is a target for cancer therapies [29]. Interestingly, while our initial phenotypic assays confirmed apoptosis induction in rRN-treated CRC cells, transcriptional changes in canonical apoptotic genes such as *BCL2*, *BAX* and Caspases (*CASP3* and *CASP8*) were not statistically significant (Supplementary **Table 1** and **Figure S1**). This suggests that rRN-induced apoptosis may occur via post-transcriptional mechanisms or as a downstream consequence of growth arrest and cellular stress triggered by cell cycle disruption. The observed suppression of *CCNB1*, *CCND1*, and *EGFR*, which are critical for proliferative signaling, could lead to irreparable cell cycle arrest, activating stress-induced apoptotic pathways independent of transcriptional regulation. For instance, caspase activation via proteolytic cleavage or post-translational modifications of BCL-2 family proteins may drive apoptosis without detectable mRNA-level changes. Future studies focusing on protein-level analyses (e.g., Western blotting for cleaved caspases, BCL-2/Bax ratios) will clarify these mechanisms and resolve the interplay between growth arrest and apoptotic signaling.

Furthermore, the significant downregulation of cell motility-related genes (*FN1*, *PXN* and *SNAI1*) highlights the ability of rRN to attenuate migratory and invasive properties, while its limited effect on *VIM* suggests partial specificity for epithelial-mesenchymal transition markers. FN1 (Fibronectin 1) is an extracellular matrix glycoprotein that plays a crucial role in cell adhesion, migration, wound healing, and tissue repair. PXN (Paxillin) is a cytoskeletal protein that acts as a scaffold for signal transduction at focal adhesions, regulating cell adhesion, migration, and cytoskeletal organization. SNAI1 (Snail Family Transcriptional Repressor 1) is a transcription factor that promotes epithelial-mesenchymal transition by repressing epithelial markers like E-cadherin and enhancing mesenchymal traits. VIM (Vimentin) is an intermediate filament protein essential for maintaining cellular integrity and providing mechanical support. Dysregulation of these proteins contributes to cancer progression by promoting epithelial-mesenchymal transition, enhancing tumor invasion, metastasis, and resistance to therapy [30].

The strong suppression of drug-resistance genes (*ABCG2*, *MRP1* and *MRP2*) in HT-29 cells and partial suppression in Caco-2 cells underscores the potential of rRN to sensitize CRC cells to chemotherapy by targeting multidrug resistance transporters. These findings align with previous studies indicating that bacteriocins can interfere with pathways critical to cancer cell survival, drug resistance, and invasion [13, 20]. ABCG2 (ATP-Binding Cassette Subfamily G Member 2), MRP1 (Multidrug Resistance-Associated Protein 1), and MRP2 (Multidrug Resistance-Associated Protein 2) are membrane transporter proteins involved in drug efflux and play significant roles in multidrug resistance in cancer. ABCG2 is crucial for expelling xenobiotics, drugs, and toxins from cells, reducing intracellular drug accumulation and decreasing chemotherapy effectiveness. MRP1 functions as an ATP-dependent efflux pump that transports various substrates, including drugs, organic anions, and glutathione conjugates, thereby lowering intracellular drug concentrations and diminishing treatment efficacy. Similarly, MRP2 is an ATP-binding cassette transporter responsible for the efflux of drugs, bilirubin, and other conjugated organic anions. Highly expressed in the liver, MRP2 contributes to bile secretion and can also promote drug resistance in cancer by exporting chemotherapeutic agents out of cells [31].

Such comprehensive suppression of cancer-driving genes reflects the effectiveness of rRN as an anticancer agent, making it a promising candidate for combination or standalone therapy [14]. The findings of this study suggest that rRN holds potential not only as an adjuvant in CRC treatment, particularly when combined with traditional chemotherapeutic agents like 5-FU [26], but also as a standalone intervention.

While these transcriptional findings highlight rRN' s therapeutic promise, further validation at the protein level is critical to fully elucidate its mechanistic underpinnings. For example, apoptosis observed phenotypically but not transcriptionally highlights the need to assess post- translational regulation (e. g. , caspase cleavage, protein- protein interactions) . Similarly, protein assays will confirm whether downregulated genes translate to functional changes in drug efflux or EMT. Addressing these gaps will not only solidify rRN' s preclinical relevance but also refine strategies for its clinical application, such as identifying synergies with chemotherapy.

However, even with robust mechanistic validation, advancing rRN to clinical translation introduces broader challenges. These include *in vivo* safety and pharmacokinetic studies, optimized delivery systems (e. g. , nanoparticle formulations) , and navigating regulatory requirements. Although standalone rRN development remains a long- term goal, combining it with low- dose 5- FU offers a near- term strategy to reduce chemotherapy toxicity while maintaining efficacy - a balance requiring rigorous optimization for both approaches. Success ultimately hinges on interdisciplinary collaboration, comparative preclinical studies, and sustained efforts to bridge scalability and real-world applicability gaps.

Conclusions

In this study, rRN was successfully expressed and purified in a soluble form that facilitates efficient future use. Functionally, rRN exhibits significant anticancer properties by selectively inhibiting CRC cell growth while sparing normal cells. Additionally, rRN enhanced the efficacy of 5- FU, suggesting a promising combination that could help reduce chemotherapy-related toxicity. Beyond its growth- inhibitory effects, rRN induced apoptosis, attenuated migration and invasion capabilities, and increased chemotherapeutic drug sensitivity by suppressing key regulatory genes involved in cancer cell proliferation, motility, and drug resistance. Collectively, our findings emphasize the therapeutic potential of rRN in CRC treatment, either as a standalone agent or in combination with existing chemotherapies. Future research should focus on exploring the precise molecular mechanisms underlying its selective anticancer activity, optimizing its production for clinical applications, and evaluating its efficacy in *in vivo* models.

Acknowledgements

This research was supported by the National Science, Research and Innovation Fund (NSRF) and Prince of Songkla University (Ref. No. SCI6701124S) to Sumalee Obchoei. Phonprapavee Tantimetta was supported by a Prince of Songkla University Ph. D. Scholarship (PSU_PHD2565-002), a Scholarship for Overseas Ph. D. Thesis Research (OTR 2568-003), and a Thesis Research Grant from the Graduate School of Prince of Songkla University, Thailand.

References

[1] F Bray, J Ferlay, I Soerjomataram, RL Siegel, LA Torre and A Jemal. Global cancer statistics 2018: GLOBOCAN estimates of incidence and mortality worldwide for 36 cancers in 185 countries. *A Cancer Journal for Clinicians* 2018; **68(6)**, 394-424.

[2] J Douaiher, A Ravipati, B Grams, S Chowdhury, O Alatise and C Are. Colorectal cancer-global burden, trends, and geographical variations. *Journal of Surgical Oncology* 2017; **115(5)**, 619-630.

[3] T Sawicki, M Ruszkowska, A Danielewicz, E Niedzwiedzka, T Arlukowicz and KE Przybylowicz. A review of colorectal cancer in terms of epidemiology, risk factors, development, symptoms and diagnosis. *Cancers* 2021; **13(9)**, 2025.

[4] H Fadlallah, J El Masri, H Fakhereddine, J Youssef, C Chemaly, S Doughan and W Abou-Kheir. Colorectal cancer: Recent advances in management and treatment. *World Journal of Clinical Oncology* 2024; **15(9)**, 1136-1156.

[5] WA Hammond, A Swaika and K Mody. Pharmacologic resistance in colorectal cancer: A review. *Therapeutic Advances in Medical Oncology* 2016; **8(1)**, 57-84.

[6] J Kaur, J Elms, AL Munn, D Good and MQ Wei. Immunotherapy for non-small cell lung cancer (NSCLC), as a stand-alone and in combination therapy. *Critical Reviews in Oncology /Hematology* 2021; **164**, 103417.

[7] TR Klaenhammer. Bacteriocins of lactic acid bacteria. *Biochimie* 1988; **70(3)**, 337-349.

[8] F De Filippis, E Pasolli and D Ercolini. The food-gut axis: Lactic acid bacteria and their link to food, the gut microbiome and human health. *FEMS Microbiology Reviews* 2020; **44(4)**, 454-489.

[9] E Pessione. Lactic acid bacteria contribution to gut microbiota complexity: Lights and shadows. *Frontiers in Cellular and Infection Microbiology* 2012; **2**, 86.

[10] A Darbandi, A Asadi, M Mahdizade Ari, E Ohadi, M Talebi, M Halaj Zadeh, A Darb Emamie, R Ghanavati and M Kakanj. Bacteriocins: Properties and potential use as antimicrobials. *Journal of Clinical Laboratory Analysis* 2022; **36(1)**, e24093.

[11] SC Yang, CH Lin, CT Sung and JY Fang. Antibacterial activities of bacteriocins: Application in foods and pharmaceuticals. *Frontiers in Microbiology* 2014; **5**, 241.

[12] M Zimina, O Babich, A Prosekov, S Sukhikh, S Ivanova, M Shevchenko and S Noskova. Overview of global trends in classification, methods of preparation and application of bacteriocins. *Antibiotics* 2020; **9(9)**, 553.

[13] S Kaur and S Kaur. Bacteriocins as potential anticancer agents. *Frontiers in Pharmacology* 2015; **6**, 272.

[14] Y Wang, Y Wang, T Sun and J Xu. Bacteriocins in cancer treatment: Mechanisms and clinical potentials. *Biomolecules* 2024; **14(7)**, 831.

[15] AM Molujin, S Abbasiliasi, A Nurdin, PC Lee, JA Gansau and R Jawan. Bacteriocins as potential therapeutic approaches in the treatment of various cancers: A review of *in vitro* studies. *Cancers* 2022; **14(19)**, 4758.

[16] SD Todorov, CM Dioso, MT Liong, LA Nero, K Khosravi-Darani and IV Ivanova. Beneficial features of pediococcus: From starter cultures and inhibitory activities to probiotic benefits. *World Journal of Microbiology and Biotechnology* 2022; **39(1)**, 4.

[17] H Zhao, R Sood, A Jutila, S Bose, G Fimland, J Nissen-Meyer and PK Kinnunen. Interaction of the antimicrobial peptide pheromone Plantaricin A with model membranes: Implications for a novel mechanism of action. *Biochimica et Biophysica Acta* 2006; **1758(9)**, 1461-1474.

[18] K Kerdkumthong, W Chanket, P Runsaeng, S Nanarong, K Songsurin, P Tantimetta, C Angsuthanasombat, A Aroonkesorn and S Obchoei. Two recombinant bacteriocins, rhamnosin and lysostaphin, show synergistic anticancer activity against gemcitabine-resistant cholangiocarcinoma cell lines. *Probiotics and Antimicrobial Proteins* 2024; **16(3)**, 713-725.

[19] YP Shih, WM Kung, JC Chen, CH Yeh, AH Wang and TF Wang. High-throughput screening of soluble recombinant proteins. *Protein Science* 2002; **11(7)**, 1714-1719.

[20] M Khaledi, HEG Ghaleh, MA Abyazi, HM Hosseini and R Golmohammadi. The anticancer properties of probiotic species. *Journal of Applied Biotechnology Reports* 2023; **10(4)**, 1123-1139.

[21] T Utsugi, AJ Schroit, J Connor, CD Bucana and IJ Fidler. Elevated expression of phosphatidylserine in the outer membrane leaflet of human tumor cells and recognition by activated human blood monocytes. *Cancer Research* 1991; **51(11)**, 3062-3066.

[22] F Schweizer. Cationic amphiphilic peptides with cancer-selective toxicity. *European Journal of Pharmacology* 2009; **625(1-3)**, 190-194.

[23] S Riedl, B Rinner, M Asslaber, H Schaider, S Walzer, A Novak, K Lohner and D Zweytick. In search of a novel target - phosphatidylserine exposed by non-apoptotic tumor cells and metastases of malignancies with poor treatment efficacy. *Biochimica et Biophysica Acta* 2011; **1808(11)**, 2638-2645.

[24] DW Hoskin and A Ramamoorthy. Studies on anticancer activities of antimicrobial peptides. *Biochimica et Biophysica Acta* 2008; **1778(2)**, 357-375.

[25] AL Hilchie, CD Doucette, DM Pinto, A Patrzykat, S Douglas and DW Hoskin. Pleurocidin-family cationic antimicrobial peptides are cytolytic for breast carcinoma cells and prevent growth of tumor xenografts. *Breast Cancer Research* 2011; **13(5)**, R102.

[26] C Cesa-Luna, JM Alatorre-Cruz, R Carreno-Lopez, V Quintero-Hernandez and A Baez. Emerging applications of bacteriocins as antimicrobials, anticancer drugs, and modulators

of the gastrointestinal microbiota. *Polish Journal of Microbiology* 2021; **70(2)**, 143-159.

[27] O Moroni, E Kheadr, Y Boutin, C Lacroix and I Fliss. Inactivation of adhesion and invasion of food-borne Listeria monocytogenes by bacteriocin-producing Bifidobacterium strains of human origin. *Applied and Environmental Microbiology* 2006; **72(11)**, 6894-6901.

[28] YC Yue, BY Yang, J Lu, SW Zhang, L Liu, K Nassar, XX Xu, XY Pang and JP Lv. Metabolite secretions of *Lactobacillus plantarum* YYC-3 may inhibit colon cancer cell metastasis by suppressing the VEGF-MMP2/9 signaling pathway. *Microbial Cell Factories* 2020; **19(1)**, 213.

[29] S Hume, GL Dianov and K Ramadan. A unified model for the G1/S cell cycle transition. *Nucleic Acids Research* 2020; **48(22)**, 12483-12501.

[30] P Nisticò, MJ Bissell and DC Radisky. Epithelial-mesenchymal transition: General principles and pathological relevance with special emphasis on the role of matrix metalloproteinases. *Cold Spring Harbor Perspectives in Biology* 2012; **4(2)**, a011908.

[31] EM Leslie, RG Deeley and SP Cole. Multidrug resistance proteins: Role of P-glycoprotein, MRP1, MRP2, and BCRP (ABCG2) in tissue defense. *Toxicology and Applied Pharmacology* 2005; **204(3)**, 216-237.

Supplementary Materials

Table 1 List of apoptotic gene primers.

Gene		Sequence (5′ to 3′)	Amplicon length (bp)
BAX	Forward:	TCAGGATGCGTCCACCAAGAAG	103
	Reverse:	TGTGTCCACGGCGGCAATCATC	
BCL2	Forward:	TGGGCCACAAGTGAAGTCAA	115
	Reverse:	CAGCCTGCAGCTTTGTTTCAT	
CASP3	Forward:	CCTGGTTCATCCAGTCGCTT	100
	Reverse:	TCTGTTGCCACCTTTCGGTT	
CASP8	Forward:	GCTGACTTTCTGCTGGGGAT	112
	Reverse:	GACATCGCTCTCTCAGGCTC	

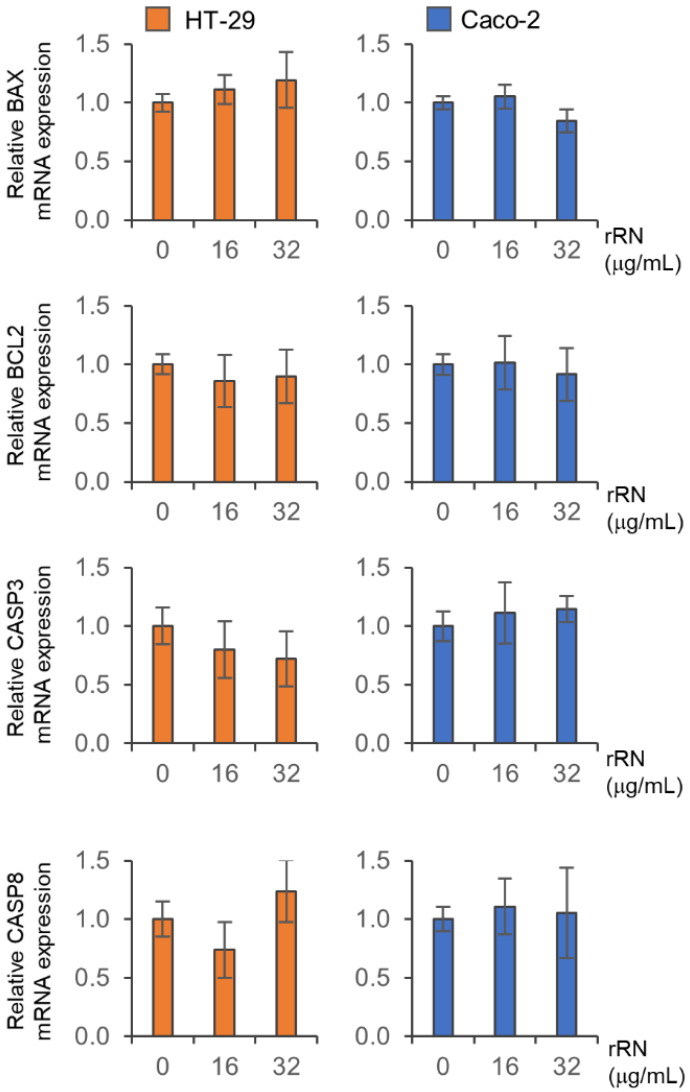

Figure S1 Gene expression analysis of apoptotic genes using RT-qPCR. Relative mRNA expression levels of apoptosis-associated genes (BAX, BCL2, CASP3 and CASP8) in rRN-treated HT-29 (orange bars) and Caco-2 cells (blue bars), as determined by RT-qPCR.